Comparisons of electric charge and axial charge meson cloud distributions in the PCQM

X. Y. Liu,[1,2,*] K. Khosonthongkee,[1] A. Limphirat,[1] P. Suebka,[1] and Y. Yan[1,†]

[1] *School of Physics, Institute of Science, Suranaree University of Technology, Nakhon Ratchasima 30000, Thailand*
[2] *School of Mathematics and Physics, Bohai University, Liaoning 121013, China*

(Dated: April 12, 2016)

The meson cloud distributions in r-space are extracted from the nucleon electromagnetic and axial form factors which are derived in the perturbative chiral quark model. The theoretical results indicate that the electric charge and axial charge distributions of the three-quark core are the same, the magnetic charge distributions of the meson cloud and three-quark core are more or less in the same region and peak at distances of around 2 GeV^{-1}, but the axial charge meson cloud distributes mainly inside the three-quark core.

PACS numbers: 12.39.Ki,14.20.-c,14.40.-n

arXiv:1601.01428v2 [hep-ph] 11 Apr 2016

I. INTRODUCTION

The meson cloud of the nucleon, undoubtedly, plays a relevant role in the study of low energy electroweak properties of the nucleon. The meson cloud model, where the nucleon is considered as a system of three valence quarks surrounded by a meson cloud [1–10], has recently been employed to study the generalized parton distribution [11, 12], nucleon electroweak form factors [13–18], nucleon strangeness [19, 20], etc. In Refs. [21–23], meson cloud contributions to the neutron charge form factor have been studied and discussed in the meson cloud model, while the effects of the meson cloud on electromagnetic transitions have been estimated in Refs. [24–26]. In our previous works [27, 28], the electromagnetic and axial form factors as well as electroweak properties of octet baryons have been studied in the perturbative chiral quark model (PCQM). The theoretical results in the PCQM with predetermined quark wave functions are in good agreement with the experimental data and lattice QCD values. In addition, Ref. [28] reveals that the meson cloud plays an important role in the axial charge of octet baryons, contributing 30%–40% to the total values, and the similar effects have been also observed in other frameworks [29, 30]. Recently, the π-meson cloud distributions of the nucleon EM form factors in r-space have been evaluated in the chiral perturbation theory [31, 32]. The results in Refs. [31, 32] show that the EM distributions peak at distances of around $r = 0.3$ fm and fall off smoothly with increasing distance. In this work, we attempt to further study and compare the meson cloud distributions of the nucleon electromagnetic and axial form factors in r-space in the framework of the PCQM.

The paper is organized as follows. In section II, we briefly describe the basic notions of the PCQM. The comparison and discussion between EM and axial form factors of nucleon are given in section III.

* lxy_gzu2005@126.com
† yupeng@sut.ac.th

II. PERTURBATIVE CHIRAL QUARK MODEL

In the framework of the PCQM, baryons are considered as the bound states of three relativistic valence quarks moving in a central Dirac field with $V_{\rm eff}(r) = S(r) + \gamma^0 V(r)$, while a cloud of pseudoscalar mesons, as the sea-quark excitations, is introduced for chiral symmetry requirements, and the interactions between quarks and mesons are achieved by the nonlinear σ model in the PCQM. The Weinberg-type Lagrangian of the PCQM under an unitary chiral rotation [14, 15] is derived as,

$$\mathcal{L}^W(x) = \mathcal{L}_0(x) + \mathcal{L}_I^W(x) + o(\vec{\pi}), \tag{1}$$

$$\mathcal{L}_0(x) = \bar{\psi}(x)\big[i\partial\!\!\!/ - \gamma^0 V(r) - S(r)\big]\psi(x) - \frac{1}{2}\Phi_i(x)\big(\Box + M_\Phi^2\big)\Phi^i(x), \tag{2}$$

$$\mathcal{L}_I^W(x) = \frac{1}{2F}\partial_\mu\Phi_i(x)\bar{\psi}(x)\gamma^\mu\gamma^5\lambda^i\psi(x) + \frac{f_{ijk}}{4F^2}\Phi_i(x)\partial_\mu\Phi_j(x)\bar{\psi}(x)\gamma^\mu\lambda_k\psi(x), \tag{3}$$

where f_{ijk} are the totally antisymmetric structure constant of $SU(3)$, the pion decay constant $F = 88$ MeV in the chiral limit, Φ_i are the octet meson fields, and $\psi(x)$ is the triplet of the u, d, and s quark fields taking the form

$$\psi(x) = \begin{pmatrix} u(x) \\ d(x) \\ s(x) \end{pmatrix}. \tag{4}$$

The quark field $\psi(x)$ could be expanded in

$$\psi(x) = \sum_\alpha \left(b_\alpha u_\alpha(\vec{x})\, e^{-i\mathcal{E}_\alpha t} + d_\alpha^\dagger \upsilon_\alpha(\vec{x}) e^{i\mathcal{E}_\alpha t}\right), \tag{5}$$

where b_α and $d_\alpha^\dagger$ are the single quark annihilation and antiquark creation operators. The ground state quark wave function $u_0(\vec{x})$ may, in general, be expressed as

$$u_0(\vec{x}) = \begin{pmatrix} g(r) \\ i\vec{\sigma}\cdot\hat{x} f(r) \end{pmatrix} \chi_s\chi_f\chi_c, \tag{6}$$

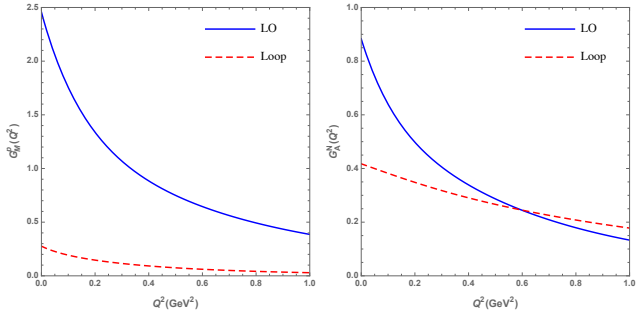

FIG. 1. Leading order (solid) and loop (dashed) contributions to the proton magnetic (left panel) form factor and neutron axial (right panel) form factor.

where χ_s, χ_f and χ_c are the spin, flavor and color quark wave functions, respectively.

In our previous works [27, 28], the ground state quark wave functions have been determined by fitting the PCQM theoretical result of the proton charge form factor $G_E^p(Q^2)$ to the experimental data [27], and the electromagnetic and axial form factors as well as electroweak properties of octet baryons in low energy region have been studied in the PCQM based on the predetermined quark wave functions. The PCQM theoretical results are in good agreement with experimental data and lattice QCD values. More details could be found in Refs. [27, 28].

III. ELECTRIC AND AXIAL CHARGE DISTRIBUTIONS OF MESON CLOUD

Following our previous works [27, 28], we present in Fig. 1 the proton magnetic and nucleon axial form factors separately in leading order (LO) and loop Feymann diagram contributions. The PCQM results shown in Fig. 1 clearly reveal that the LO diagram results in a dipole-like form factor while the meson cloud leads to a flat contribution to the magnetic and axial form factors. The flat contribution may indicate that the meson cloud of the nucleon may distribute mainly in a very small region.

In general, the form factor $F(q^2)$ is the Fourier transformation of charge distribution in r-space and takes the form,

$$F(q^2) = \int \rho(\vec{r}) e^{-i\vec{q}\cdot\vec{r}} d^3\vec{r}, \tag{7}$$

where $\rho(\vec{r})$ is the charge density, and $\vec{q}$ is the three-momentum transfer. If $F(q^2)$ has been determined, in principle, the charge distribution $\rho(r)$ could be obtained by the inverse Fourier transformation,

$$\rho(\vec{r}) = \frac{1}{(2\pi)^3} \int F(q^2) e^{i\vec{q}\cdot\vec{r}} d^3\vec{q}. \tag{8}$$

In this work, we extract, based on the inverse Fourier transformation in Eq. (8), the magnetic charge and axial charge meson cloud distributions of the nucleon from the EM and axial form factors as shown in Fig. 1. Shown in Fig. 2 are the LO and meson cloud contributions to the proton magnetic form factor $G_M^p(Q^2)$ (left panel) and the nucleon axial form factor $G_A^N(Q^2)$ (right panel) in r-space. It is found in Fig. 2 that the magnetic charge distributions of the three-quark core and the meson cloud are almost in the same region, but the loop diagrams contribute to the $G_A^N(Q^2)$ in a clearly smaller region than the LO diagram, which may indicate that the axial charge meson cloud distributes mainly inside the three-quark core.

We also find that the magnetic charge distribution shown in the left panel of Fig. 2 present a significant peak around $r \simeq 2$ GeV^{-1} and fall off smoothly when the distance increases. The results turned out to be similar to the ones of Refs. [31, 32].

Furthermore, we compare the LO contributions to the $G_M^p(Q^2)$ and $G_A^N(Q^2)$ in r-space, as presented in the left panel of Fig. 3. It is clear that the LO $G_M^p(r^2)$ and $G_A^N(r^2)$ show a similar r-dependence, which may indicate that the electric charge and axial charge distributions of the constituent quarks are the same. The meson cloud $G_M^p(r^2)$ and $G_A^N(r^2)$ in the right panel of Fig. 3 show that the axial charge distribution of the meson cloud is narrower and the peak is closer to the origin.

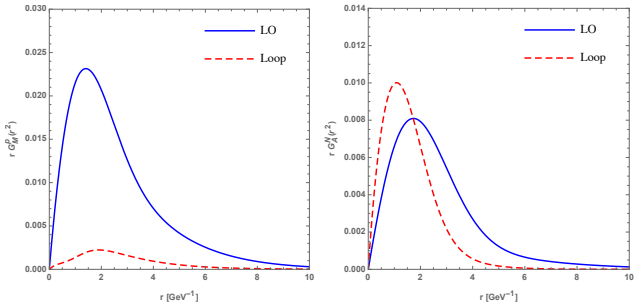

FIG. 2. Comparisons between the LO and meson cloud distributions for proton magnetic (left panel) and axial (right panel) form factors in r-space.

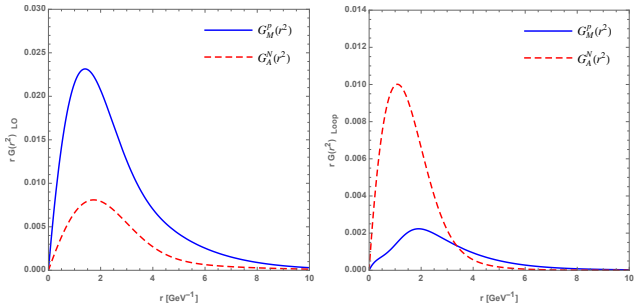

FIG. 3. Comparisons between the magnetic and axial distributions in r-space for the LO (left panel) and loop (right panel) diagrams.

In summary, one may conclude that the similar r-dependence of the magnetic and axial form factors resulted from the LO diagrams may indicate that the electric charge and axial charge distributions of the constituent quarks are the same. The magnetic charge distributions of the meson cloud and three-quark core are more or less in the same region and peak at distances of around 2 GeV^{-1}, but the axial charge meson cloud distributes mainly inside the three-quark core.

ACKNOWLEDGMENTS

This work is supported by Suranaree University of Technology and Bohai university. XL and AL acknowledge support by SUT-CHE-NRU (Project No. NV12/2558). This work is supported also by National Natural Science Foundation of China (Project No. 11547182), and the Doctoral Scientific Research Foundation of Liaoning Province (Project No. 201501197).

[1] S. Théberge, A. W. Thomas, and G. A. Miller, Phys. Rev. D **22**, 2838 (1980).
[2] A. W. Thomas, S. Théberge, and G. A. Miller, Phys. Rev. D **24**, 216 (1981).
[3] S. Chin, Nucl. Phys. A **382**, 355 (1982).
[4] E. Oset, R. Tegen, and W. Weise, Nucl. Phys. A **426**, 456 (1984).
[5] T. Gutsche and D. Robson, Phys. Lett. B **229**, 333 (1989).
[6] Z. Dziembowski, H. Holtmann, A. Szczurek, and J. Speth, Ann. Phys. **258**, 1 (1997).
[7] J. Speth and A. Thomas, Adv. Nucl. Phys. **24**, 83 (2002).
[8] A. Faessler, T. Gutsche, V. E. Lyubovitskij, and K. Pumsa-ard, Phys. Rev. D **73**, 114021 (2006).
[9] B. Juliá-Díaz and D. Riska, Nucl. Phys. A **780**, 175 (2006).
[10] D. Chen, Y. Dong, M. Giannini, and E. Santopinto, Nucl. Phys. A **782**, 62 (2007).
[11] B. Pasquini and S. Boffi, Phys. Rev. D **73**, 094001 (2006).
[12] B. Pasquini and S. Boffi, Nucl. Phys. A **782**, 86 (2007).
[13] V. E. Lyubovitskij, T. Gutsche, and A. Faessler, Phys. Rev. C **64**, 065203 (2001).
[14] V. Lyubovitskij, T. Gutsche, A. Faessler, and R. V. Mau, Phys. Lett. B **520**, 204 (2001).
[15] K. Khosonthongkee, V. E. Lyubovitskij, T. Gutsche, A. Faessler, K. Pumsa-ard, S. Cheedket, and Y. Yan, J. Phys. G: Nucl. Part. Phys. **30**, 793 (2004).
[16] B. Pasquini and S. Boffi, Phys. Rev. D **76**, 074011 (2007).
[17] G. Ramalho and K. Tsushima, Phys. Rev. D **84**, 054014 (2011).
[18] G. Ramalho, K. Tsushima, and A. W. Thomas, J. Phys. G: Nucl. Part. Phys. **40**, 015102 (2013).
[19] F. Carvalho, F. S. Navarra, and M. Nielsen, Phys. Rev. C **72**, 068202 (2005).
[20] H. Chen, F. G. Cao, and A. I. Signal, J. Phys. G: Nucl. Part. Phys. **37**, 105006 (2010).
[21] D. Lu, K. Tsushima, A. Thomas, A. Williams, and K. Saito, Phys. Lett. B **441**, 27 (1998).
[22] L. Glozman and D. Riska, Phys. Lett. B **459**, 49 (1999).
[23] J. A. Rinehimer and G. A. Miller, Phys. Rev. C **80**, 025206 (2009).
[24] G. Ramalho, D. Jido, and K. Tsushima, Phys. Rev. D **85**, 093014 (2012).
[25] G. Ramalho and K. Tsushima, Phys. Rev. D **88**, 053002 (2013).
[26] G. Ramalho and M. T. Peña, Phys. Rev. D **89**, 094016 (2014).
[27] X. Y. Liu, K. Khosonthongkee, A. Limphirat, and Y. Yan, J. Phys. G: Nucl. Part. Phys. **41**, 055008 (2014).
[28] X. Y. Liu, K. Khosonthongkee, A. Limphirat, P. Suebka, and Y. Yan, Phys. Rev. D **91**, 034022 (2015).
[29] J. Franklin, Phys. Rev. D **66**, 033010 (2002).
[30] G. Ramalho and K. Tsushima, arXiv:1512.01167 [hep-ph] (2016).
[31] H. W. Hammer, D. Drechsel, and U. G. Meißner, Phys. Lett. B **586**, 291 (2004).
[32] U. G. Meißner, AIP Conf. Proc. **904**, 142 (2007).